April 2010

A Novel Role of the p53 Tumor Suppressor Pathway in Maintaining Glucose Homeostasis

Debra-Ann Franck
Worcester Polytechnic Institute

Laura Ann Tracy
Worcester Polytechnic Institute

MQP-BIO-DSA-1390
MQP-BIO-DSA-3895

A NOVEL ROLE OF THE p53 TUMOR SUPPRESSOR PATHWAY IN MAINTAINING GLUCOSE HOMEOSTASIS

A Major Qualifying Project Report

Submitted to the Faculty of the

WORCESTER POLYTECHNIC INSTITUTE

in partial fulfillment of the requirements for the

Degree of Bachelor of Science

in

Biology and Biotechnology

by

Debra Franck Laura Tracy

April 29, 2010

APPROVED:

Hayla Sluss, Ph.D.
Program in Medicine
UMASS Medical Center
Major Advisor

David Adams, Ph.D.
Biology and Biotechnology
WPI Project Advisor

ABSTRACT

Type II diabetes is a disorder that affects the ability of the body to produce or utilize insulin, and is characterized by hyperglycemia. The p53 tumor suppressor signaling pathway has been shown to play a role in maintaining glucose homeostasis in a process mediated by Ser18. To better understand insulin resistance, we utilized a loss of p53 function model (phosphorylation mutant p53Ser23Ala) and a model where p53 is hyperactivated (model p44) to further define the role of p53 in insulin sensitivity *in vivo*. Insulin-mediated Akt activation was analyzed in various tissues as a marker for insulin sensitivity. Glucose homeostasis was measured through glucose and insulin tolerance tests. It was found through these mouse models that p53 plays a vital role in regulating glucose homeostasis and insulin sensitivity.

TABLE OF CONTENTS

ACKNOWLEDGEMENTS

First and foremost, we would like to thank Hayla Sluss, PhD., for allowing us to work in her lab at UMass Medical School. She provided guidance in forming our project's purpose, and helped edit our final report. We are especially grateful for the use of Dr. Sluss's constructs, reagents, and numerous supplies. Also, we would not have succeeded without the assistance and patience of Heather Armata in teaching us all of the lab techniques used in this MQP, as well as the day-to-day support, inspiration, and advice she gave throughout the experimentation process. We would like to thank Dr. Heidi Scrable from the University of Virginia School of Medicine, for allowing the Sluss lab to use her p44 mouse model, and Dr. Tyler Jacks from the Massachusetts Institute of Technology, Center for Cancer Research, for allowing the Sluss lab to use his p53Ser23A mutant mouse strain. Additionally, we would like to thank the Davis Lab for use of their RT-PCR machine. Last but not least, we would like to say thank you to Professor David Adams for helping initiate this MQP, giving us advice along the way, and for editing the final MQP report. This project would not have been possible without the assistance of the aforementioned individuals.

BACKGROUND

Diabetes and Glucose Dysregulation

Diabetes is a glucose dysregulation disease in which glucose is not taken up into cells of the body, resulting in serum hyperglycemia. In Type 1 diabetes, the lack of glucose uptake results from the diminished production of insulin by pancreatic beta cells. Insulin normally facilitates glucose uptake by binding insulin receptors to initiate signal transduction pathways to upregulate glucose receptors, such as GLUT-1, on the cell surface. Without insulin production, GLUT-1 is not upregulated, glucose is not taken inside the cells, and serum glucose becomes elevated.

Type 2 diabetes is the most common form of diabetes, and is one of the main causes of mortality worldwide (Kahn and Saltiel, 2001). With this type of diabetes, the cells are considered insulin-resistant which is also coupled with glucose intolerance. Insulin-resistance occurs when the body does not respond to insulin. The problem is generally "post receptor", meaning the pancreatic beta cells produce and secrete insulin, and the insulin binds insulin receptors, but the cells do not respond to the insulin binding. Glucose intolerance occurs when the produced insulin cannot initiate the metabolism of glucose into glycogen in the body's liver and muscle cells, leading to the hyperglycemia. During glucose dysregulation, several areas of the body become detrimentally affected, especially the eyes, kidneys, nerves, and heart. Type 2 diabetes is more prevalent in obese people, and is more common in African Americans, Latinos, Native Americans, and Asian Americans/Pacific Islanders, as well as the elderly population (American Diabetes Association, 2010).

An important aspect of Type 2 diabetes is the inability of the body to maintain glucose homeostasis. The normal body is able to maintain a constant plasma glucose level between 4 and 7 mM (72 to 126 mg/dL) either during or between periods of glucose ingestion. This tight homeostasis is maintained by absorption in the intestine and uptake of the glucose by the surrounding tissues. **Figure 1** summarizes how insulin regulates glucose uptake, production, and storage. Insulin increases glucose uptake into cells by binding the insulin receptor (blue in the diagram) to upregulate glucose transporters, such as GLUT-1 (red in the diagram). Glucose transporters bind glucose transporting it across the cell membrane. Insulin binding to its receptor also increases the uptake of amino acids using their amino acid transporters (green). Glucose brought into the cell is converted to triglycerides, glycogen, or enters glycolysis (red arrows). Prolonged binding of insulin to its receptor subsequently inhibits glucose production by those cells, and inhibits the conversion of triglycerides to fatty acids. Thus, insulin serves as a powerful glucose homeostasis regulator (Kahn and Saltiel, 2001).

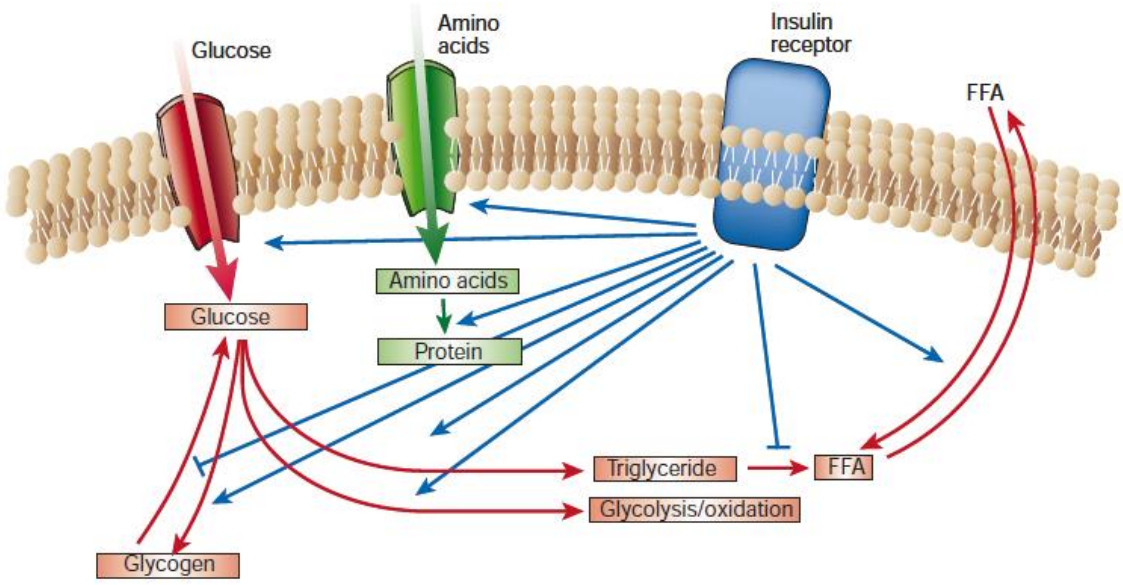

Figure 1. Summary of Glucose Homeostasis by Insulin. Insulin regulates glucose uptake and production, and promotes the synthesis and storage of carbohydrates, lipids and proteins (Kahn and Saltiel, 2001).

Many tissues in the body assist in glucose regulation **(Figure-2)**. After glucose is absorbed through the intestine, the beta cells of the pancreas secrete insulin in response to the elevated plasma glucose levels. The principle role of the hormone insulin is to control the plasma glucose concentrations through stimulating glucose transport into muscle and fat cells, and reducing glucose output from the liver (Ogawa et al., 1998). As discussed above, insulin also causes a decrease in liver glucose production (from stored glycogen) and increases the level of glucose uptake in the liver, initiating its conversion into glycogen. It is essential to store glucose as glycogen because the glycogen molecule is small, less reactive than glucose, and is insoluble in water, meaning it will not affect the osmotic levels and pressure of the cells that store it. When energy is needed, the glycogen store in liver cells can be converted back into glucose and distributed to the entire body. This glycogen conversion also occurs when insulin levels are low or absent, triggering an unnecessarily high amount of glucose to convert from glycogen, leading to

a state of cellular hyperglycemia. Insulin also increases glucose storage, as glycogen, in fat and muscle cells. The glycogen produced in the muscle cells serves as an immediate energy source for these muscle cells only, and is not distributed throughout the body because these cells lack the necessary enzymes that allow the glucose to enter into the blood. Fat cells release FFAs (free fatty acids) which cause a decrease in glucose uptake in muscle cells, a decrease in insulin secretion and increased glucose production from the liver. FFAs derived from adipocytes are found to be elevated in the serum in insulin-resistant organisms. This suggests that this is a contributing factor to the insulin resistance of diabetes, causing obesity by inhibiting glucose uptake and glycogen synthesis. This link may also suggest that the accumulation of triglycerides and fatty acid metabolites in muscle and liver are involved in insulin resistance (Ogawa et al., 1998; Kahn and Saltiel, 2001).

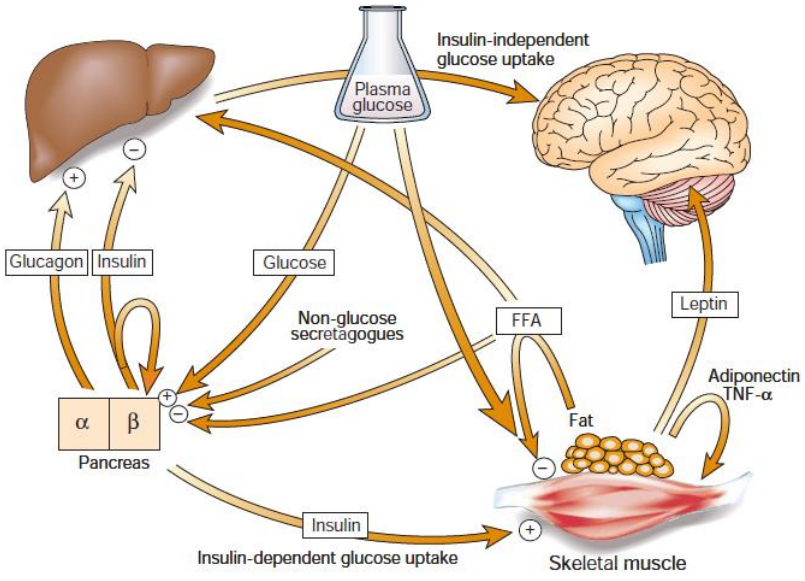

Figure 2: Role of Different Organs in Glucose Homeostasis. Diagram illustrates the interaction of various body systems and tissues in the regulation of glucose homeostasis through glucose uptake and insulin secretion (Kahn and Saltiel, 2001).

The Insulin Receptor

Insulin is the main hormone controlling essential energy functions, including glucose and lipid metabolism. Insulin elicits a variety of biological responses once bound to its receptor (SABiosciences, 2009). Insulin receptors are part of the receptor tyrosine kinase subfamily that also includes insulin-like growth factor (IGF-I) receptor and the insulin receptor-related receptor (IRR). These tetrameric proteins consist of two alpha subunits and two beta subunits. The alpha subunit inhibits the tyrosine kinase activity of the beta subunit. The insulin receptor, along with the IGF-I and IRR receptors, are also able to form functional hybrids. If an inhibitory mutation arises in one of the receptors, it may affect the activity of the other two due to the formed hybrids (Kahn and Saltiel, 2001; SABiosciences, 2009). When insulin binds the insulin receptor on the surface of the cell it initiates several signal transduction pathways involving a variety of protein kinase molecules, whose result was shown as blue arrows in **Figure 1**: upregulation of the GLUT1 transporter, increased conversion of glucose to glycogen, and increased usage of glucose in glycolysis. Insulin mediates these effects via activation of signaling pathways (**Figure 3)** which utilize: adaptor molecules such the IRS (Insulin Receptor Substrates), the SHC (Src and Collagen Homologues) and the GRB2 (Growth Factor Receptor Binding protein-2); lipid kinases such as PI3K (Phosphatidylinositol 3-Kinase); small G-proteins like Rac; and serine, threonine and tyrosine kinases (Ogawa et al., 1998).

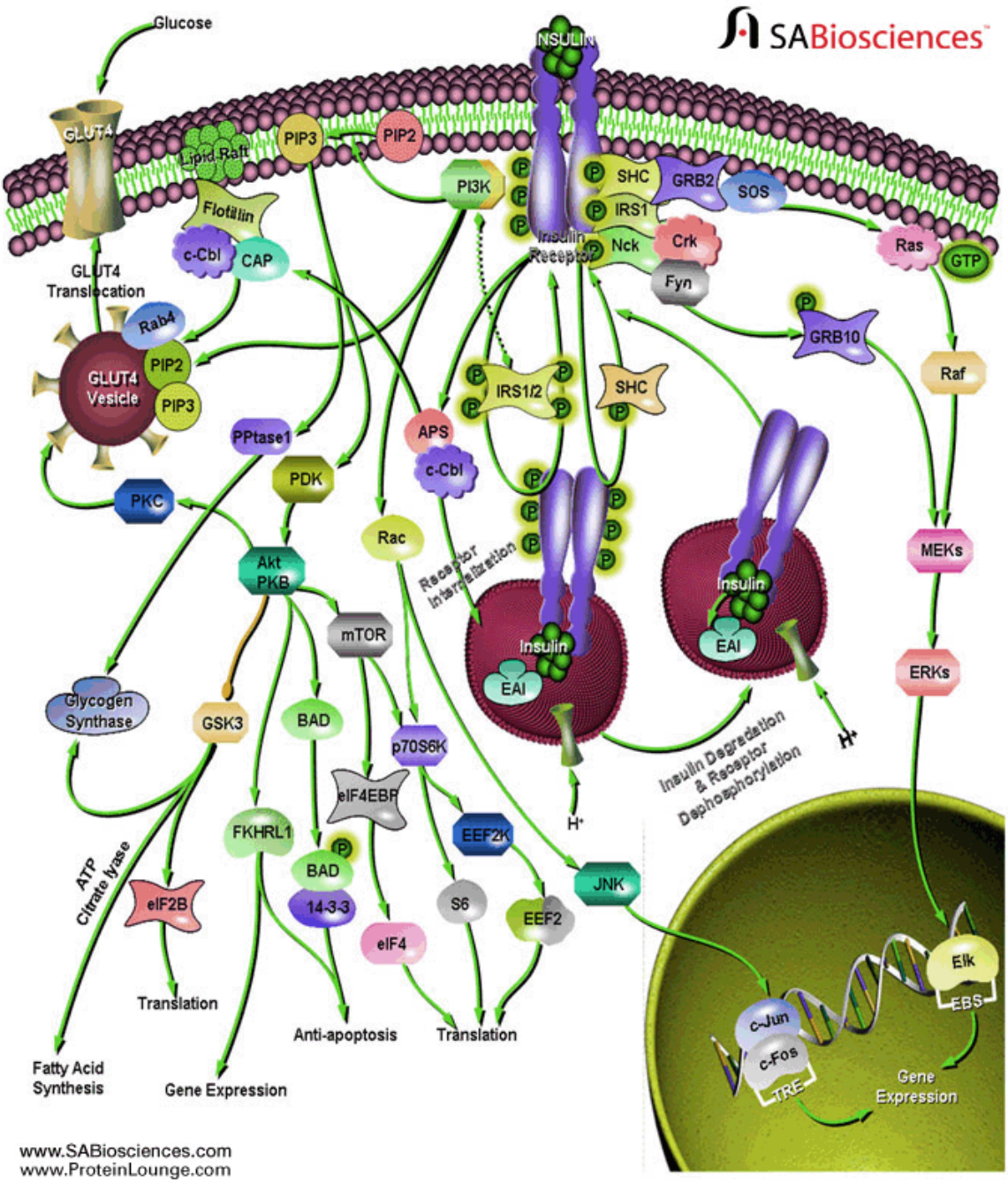

Figure 3. Summary of Kinase Activation in the Presence of Insulin. Activation of the insulin receptor via insulin causes a cascade of biological effects on cells including stimulation of glucose transport, gene expression and alterations of cell morphology (SABiosciences, 2009).

One key pathway in insulin signal transduction is the Akt kinase pathway. The serine/threonine kinase Akt, also known as protein kinase B (PKB), is a central node in cell signaling downstream of growth factors, cytokines, and other cellular stimuli. Abnormal loss or gain of Akt activation is an underlying cause of the physiological properties of a variety of complex diseases, including type-2 diabetes and cancer (Manning and Cantley, 2007).

Akt Pathway

The Ser/Thr kinase Akt/Protein Kinase B pathway is highly conserved across a wide range of species, and is involved in many cellular processes. Though it is has many roles, an important aspect of the Akt pathway is its role in regulating the metabolic effects of insulin in several target tissues. **Figure 4** summarizes the effect of the Akt pathway (up-regulation or down-regulation) in four insulin-responsive metabolic tissues. The role of Akt is not completely understood in the coordination of insulin action throughout the body, but Akt is known to be a key regulator of the insulin-signaling pathway that plays a role in glucose homeostasis (Whiteman et al., 2002). Any disruption in the Akt pathway would lead to insulin resistance and glucose dysregulation, so understanding this pathway is important when studying of Type 2 diabetes.

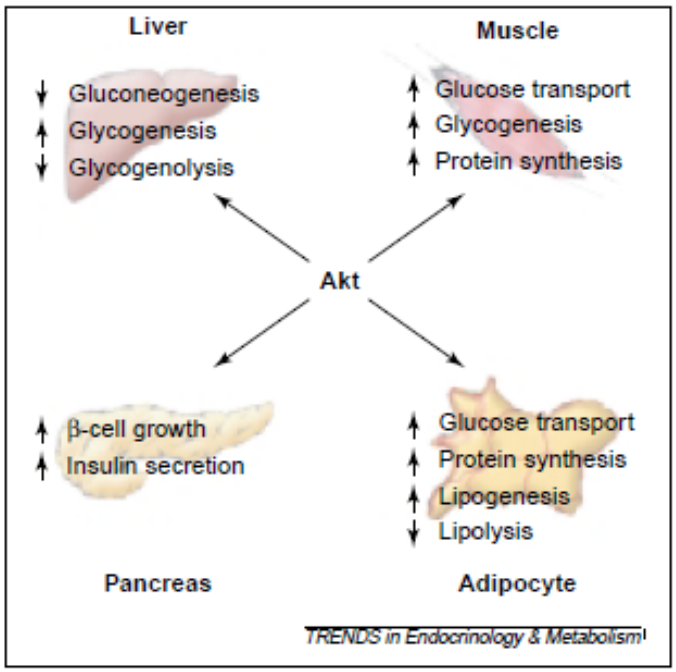

Figure 4: Summary of the Effects of the Insulin-Induced Akt Kinase Pathway. Shown are the events up-regulated and down-regulated in insulin responsive metabolic tissues following activation of the Akt kinase pathway by insulin binding its receptor (Whiteman et al., 2002).

p53 Functions

The p53 tumor suppressor has an important role in gene expression and genetic stability. In almost fifty percent of all human cancers, p53 is mutated, causing an accumulation of DNA mutations, and the expression of dysfunctional cellular proteins (Steele et al., 1998). Many studies have shown that p53 is stressed-induced, and it functions by restricting the proliferation of abnormal cells (Kubbutat,1997; Olovnikov et al., 2008). However, more recent studies have suggested that p53 also plays a role in cells under *non-stress* situations. For example, p53 has been shown to contribute to the homeostatic regulation of different metabolic processes (Olovnikov et al., 2008). p53 acts as a transcription factor, and previous studies have shown that more than 500 genes are potentially regulated by p53 (Olovnikov et al., 2008).

p53 is found to be expressed in multiple tissues in mice, including brain, pancreas, liver, muscle, and adipose tissue, many of which are involved in glucose homeostasis. In addition to blocking cell division (for abnormal cells), the p53 pathway has also been noted to affect cellular metabolism. Hyperglycemia has been shown to activate p53 and induce its phosphorylation (Schmitt et al., 1999) (**Figure 5**). Shown in the diagram are two key phosphorylation sites (Ser18 and Ser23) located within the transactivation domain on the N terminal of the gene. Other studies have correlated p53 with aging, age-related insulin resistance, and diabetes (Rudolph et al., 1999).

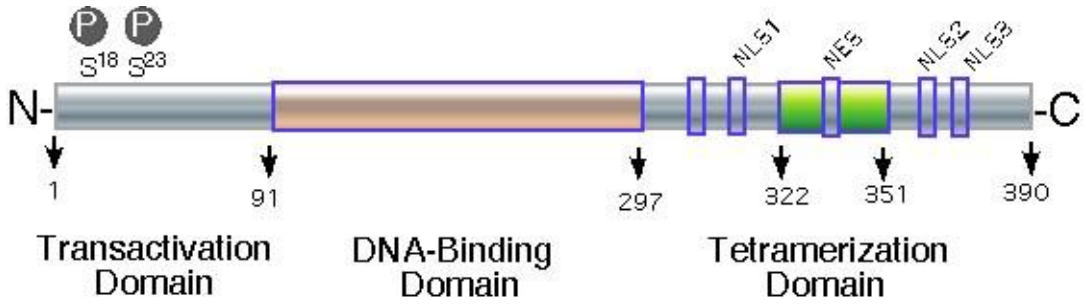

Figure 5: Diagram of the Murine p53 Transcription Factor Protein. Shown are the major domains of p53 protein, including its N-terminal transactivation domain on which the *Ser18* and *Ser 23* phosphorylation sites reside. Also shown are its DNA-binding domain (diagram center), and its tetramerization domain which helps form complexes with other p53 molecules.

Research has linked p53 with the control of the Warburg effect in tumor cells (Luo et al., 2004). The Warburg effect is described in cancer cells as increased glycolysis even when sufficient glucose is present. Cells from p53-deficient mouse models show a decreased oxidative phosphorylation with an increased glycolysis (Macpherson et al., 2004). Thus, p53 plays a role in regulating glucose homeostasis.

Ataxia Telangiectasia and the Sluss Lab Studies

The Sluss Laboratory at Umass Medical School has performed research on Ataxia telangiectasia (A-T). In this disease, patients can develop multiple clinical pathologies, including neuronal degeneration, elevated risk of cancer, telangiectasias, and growth retardation (Spring et al., 2002; Lavin, 2008). A-T patients may demonstrate an increased risk of insulin resistance and Type 2 diabetes (Bar et al., 1978). ATM is a protein kinase mutated in some A-T patients, and has been implicated in metabolic diseases including insulin resistance (Shoelson, 2006). ATM phosphorylates p53 on a site that regulates transcriptional activity (Sluss et al., 2004).

The Sluss Laboratory has studied the p53 *Ser18* phosphorylation site for the regulation of glucose homeostasis using a p53Ser18A mouse model. Mice are the most commonly used vertebrate species used for *in vivo* studies and are considered to be a prime model of inherited human disease because they share 99% of their genes with humans. Because the ATM gene is mutated in some A-T patients, and this mutation correlates with insulin resistance, and ATM normally phosphorylates p53 at a site known to regulate transcriptional activity (Sluss et al., 2004), the next step for the Sluss laboratory was to test whether ATM regulates insulin-resistance through p53 phosphorylation. **Figure 6** is a model of the p53 pathway in cell cycle checkpoint control. Note that DNA damage leads to phosphorylation of p53 on *Ser18* and *Ser23* by the ATM/ATR signaling pathway. A single phosphorylation of each site regulates different aspects of the p53 functions (shown as X, Y, and Z).

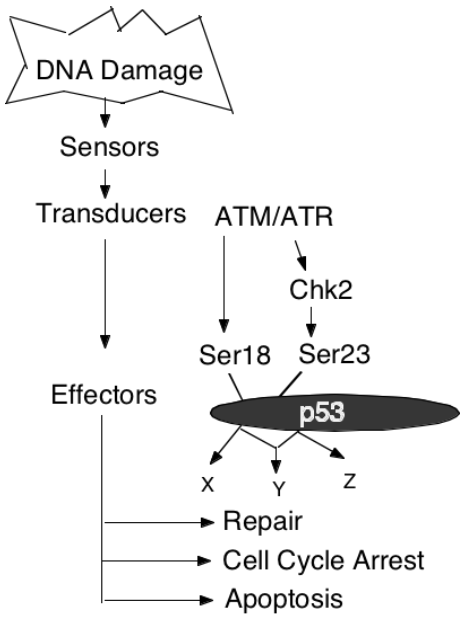

Figure 6: Diagram of the p53 Pathway Cell Cycle Checkpoint Controls. DNA damage is recognized by sensor proteins that relay the signal to transducers and lead to effectors that mediate a cellular response. DNA activation leads to phosphorylation of p53 on Ser18 and Ser23 by the ATM/ATR signaling pathway. A phosphorylation at either site regulates different aspects of p53 function (Sluss, personal communication).

Sluss Laboratory p53Ser18Ala Mouse Model

The Sluss Laboratory studied insulin sensitivity in a mouse model in which the p53 phosphorylation site *Ser18* was replaced with alanine (this site it highlighted with a red box in **Figure 7**). The lack of phosphorylation at this p53 site was shown to increase metabolic stress and cause severe defects in glucose homeostasis compared to a wildtype mouse. The p53Ser18Ala model also showed glucose intolerance and insulin resistance. Thus, the mouse model showed that p53 phosphorylation on a site known to be regulated by ATM is an important mechanism in the physiological regulation of glucose homeostasis (Sluss, personal communication).

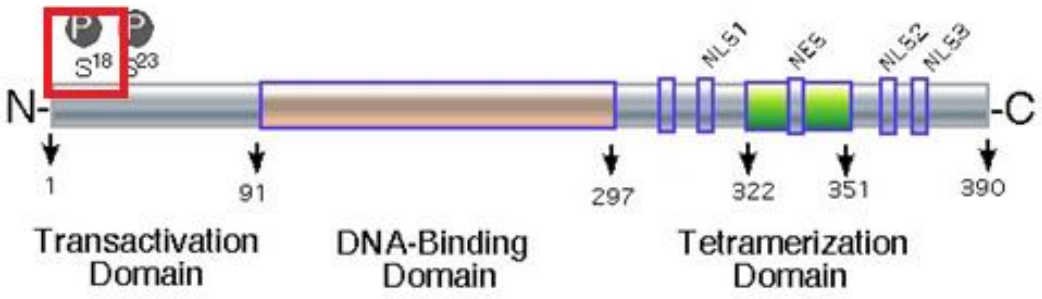

Figure 7: Diagram of the Murine p53 Transcription Factor Showing the Phosphorylation Site Mutated in a Mouse Model. The p53 N-terminal *Ser18* phosphorylation site (shown by a red box) was replaced with alanine in the p53Ser18Ala mouse model.

Mouse Models Used in This Project

p53Ser23Ala

Two mouse models were utilized in this project, p53Ser23Ala and p44. p53Ser23Ala was the first model investigated in this project. The p53 *Ser23* phosphorylation site has been proposed to work in conjunction with the previously studied *Ser18* phosphorylation site, so a p53Ser23Ala mouse mutant was chosen for analysis. This model was originally created by Dr. Tyler Jacks, at MIT (Macpherson et al., 2004). **Figure 8** is a diagram of the p53Ser23A mutation, with the mutation site highlighted by the red box. The murine p53Ser23 phosphorylation site is homologous to the p53Ser20 phosphorylation site in humans. The p53Ser23 site is also part of the ATM/ATR signaling pathway, and it is proposed that p53Ser23 may work in conjunction with p53Ser18 to regulate the function of p53. Though these two sites could work in conjunction, they will be studied individually; the Sluss lab has already investigated the functions of p53Ser18A, so this project will focus on the p53Ser23A model to determine whether the mutation has an effect on the development of insulin resistance and glucose intolerance.

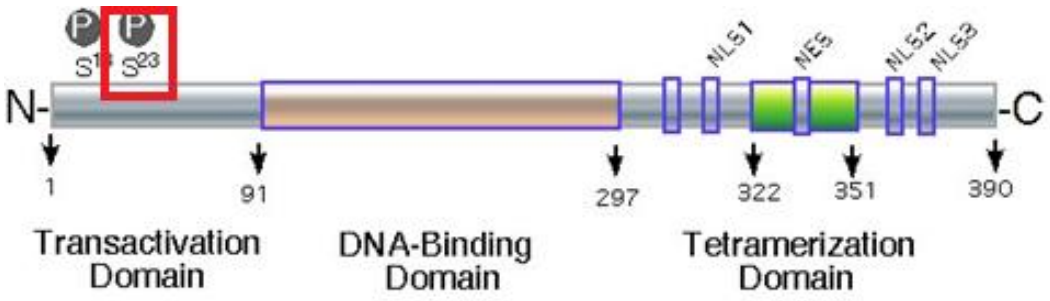

Figure 8: Diagram of Murine p53 Transcription Factor Mutated at the *Ser23* Phosphorylation Site. The mutation site is shown by a red box. Serine has been replaced with an alanine to produce the p53Ser23Ala mutant mouse model used in this project.

p44 Mouse Model

The second model used in this project is p44. This model was originally created by Dr. Heidi Scrable at the University of Virginia School of Medicine (Scrable et al., 2005). p44 is a truncated form of p53 that binds to p53 to make a dimer increasing its activity. **Figure 9** is a diagram of the p44 Transgene; the red box indicates the alternative translation start site at codon 41 located in the transactivation domain of the murine p53 transcription factor. p44 is a p53 homolog resembling a shorter p53 isoform. Both human and murine p44 lack part of the N-terminal region present in full length p53 (Scrable, 2004). p44 is naturally found at low levels in both mice and humans, and the genomic structure of the mouse p44 gene is identical to the structure of the human p44 gene, indicating a this gene is highly conserved throughout evolution (Garcia et al., 1998). It is thought that p44 interacts with p53 in mammals by enhancing its ability to suppress cell proliferation, however the functions of p44 are not yet fully understood. The overexpressed p44 transgenic mice created by Maier et al. (2004) shows signs of premature aging and are half the size of their non-transgenic littermates (Campisi, 2004).

The activity of p53 is thought to be elevated in p44 mice. The transgenic mice have a very low occurrence of cancer development (an attribute of up-regulated p53). These findings support the thought that hyperactive p53 can cause accelerated aging, and p44 aids in this activity (Campisi, 2004). We will be studying the effects of the overexpression of p53 caused by the p44 transgene model to understand whether this overexpression has an effect on the development of insulin resistance and glucose intolerance.

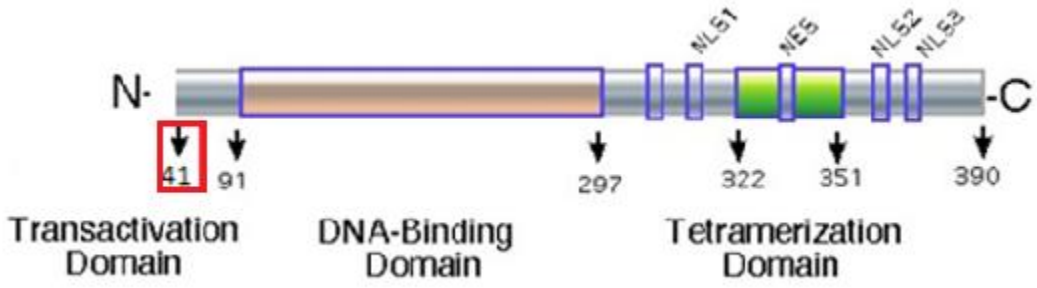

Figure 9: Diagram of the p44 Transgene. Figure shows a homolog of p53 used in the p44 transgenic mouse models. The gene has a truncated transactivation domain, and is known to hyperactivate p53 transcription factor.

Both mouse models will be extensively studied to obtain data about potential alterations in glucose homeostasis. The observations will be compared to a wildtype strain used as a control to verify all results. The hope is that the two models will provide data showing whether the p53Ser23Ala phosphorylation site, and/or an increased p53 activity for the p44 transgene, play a role in glucose homeostasis, and whether they affect the p53 transcription factor significantly in its role as a glucose regulator.

PROJECT PURPOSE

Type 2 diabetes is a disorder characterized by glucose dysregulation contributed by insulin resistance. Understanding the mechanism of pre-diabetic insulin resistance would provide a critical step towards identifying the early stages of the development of diabetes. The potential role of p53 tumor suppressor in regulation of glucose homeostasis and insulin sensitivity is suspected but not proven. The proposed studies will examine the mechanisms underlying insulin resistance in two transgenic mouse strains, p53Ser23Ala (expressing a mutated p53 that can not be phosphorylated at the Ser23 site) and p44 (expressing a truncated form of p53 that forms dimers with p53 increasing its activity). These studies are an extension of the Sluss Laboratory's previous findings that p53Ser18Ala mice (mutated at a different site) developed glucose intolerance and insulin resistance. The purpose of this research is to help define the contribution of the p53 signaling pathway in glucose homeostasis, insulin signaling, and Type 2 diabetes. Insulin sensitivity and Akt pathway-insulin sensitivity in each mouse model will be monitored by Glucose and Insulin Tolerance Tests. The mice will then be sacrificed, and protein and RNA will be purified from liver, muscle, and white fat tissues. Protein expression of the Akt pathway will be monitored by immunoblots, and RT-PCR will show relative mRNA expression in these tissues. This project was completed as part of the Sluss Laboratory's long term goal of defining the contribution of the p53 signaling pathway in glucose homeostasis, insulin signaling, and Type 2 diabetes.

METHODS

Mouse Models

Mouse Model Strains

The p53Ser23A mutant mouse strain was generously donated by Dr. Tyler Jacks, Center for Cancer Research, Massachusetts Institute of Technology. The p44 transgenic strain was generously donated by Dr. Heidi Scrable, Department of Neuroscience, University of Virginia School of Medicine. The mice were housed in specific pathogen-free facilities accredited by the American Association for Laboratory Animal Care. The Institutional Animal Care and Use Committee (IACUC) of the University of Massachusetts Medical School approved all studies using these animals.

Animal Husbandry

Mice were handled in accordance with IACUC's policy on the maintenance of mouse breeding colonies. Gloves, hair net, face mask, shoe covers, and body suit were utilized when entering the mouse room area. The specific animal husbandry methods followed include: specified weaning dates (21 days old), no more than 1 litter per cage, no more than 5 mice per cage, separate males and females, and appropriate breeding (same strains). When sacrificed, mice were double killed in accordance with IACUC policy.

Glucose Tolerance Tests

Mice were fasted overnight, then challenged by intraperitoneal administration of glucose (1g/kg body weight, IMS). Glucose levels were determined at 0, 15, 30, 45, 60

and 120 min after glucose stimulation. Blood glucose was measured with an Ascenzia Breeze 2 glucometer (Bayer).

Insulin Tolerance Tests

Mice were fasted overnight, then challenged by intraperitoneal administration of insulin (0.75 units/kg body weight, Sigma, St. Louis, MO). Glucose levels were determined at 0, 15, 30, 60, 90 and 120 min after insulin stimulation. Blood glucose was measured with an Ascenzia Breeze 2 glucometer (Bayer).

Tissue Harvesting and Storage

Mice were sacrificed in accordance with IACUC standards (double kill policy). Animals were immediately dissected, and target tissues and organs (liver, muscle, pancreas, spleen, white fat) were harvested, placed on 6 well plates, and frozen on dry ice. Tissues were stored at -80°C.

Mouse Genotyping

Tail Section Digestion

A 1.0-1.5 cm section of mouse tail was cut and added to 700 µL of Lysis Buffer (50 mM Tris pH 7.5, 50 mM EDTA pH 8.0, 100 mM NaCl, 5 mM DTT, 0.5 mM Spermidine, and 1% SDS). 20 µL of freshly prepared 20 mg/ml Proteinase K (in sterile water) was added to each tube, then the tubes were shaken gently overnight, at 55°C.

DNA Isolation

The eppendorf tubes were then spun at max speed for 5 minutes to pellet any tissue debris. The supernatant (containing DNA) was collected, and an equal volume of

phenol/chloroform/iso-amyl alcohol mix (25:24:1) was added. Tubes were mixed by hand and then spun at max speed for 5 minutes. The aqueous (top) phase of each tube was collected, and an equal volume of absolute ethanol was added to tube, DNA was precipated by gentle inversion of the tubes. The DNA samples were rinsed once with 80% EtOH, and let air dry. An aliquot of 50-100 µL of TE was added to the DNA pellet, and dissolved overnight at room temperature. The DNA was stored at 4°C.

PCR

The PCR consisted of making up a master mix solution that included Nuclease-Free water (to final volume of 50 µl), 5x Green GoTaq® buffer, dNTP mix, GoTaq® DNA Polymerase (5U/µl), 25 mM $MgCl_2$, and gene specific downstream and upstream primers. The primers used for the p53Ser23A mice (MacPherson, 2004) were: 5'-AGCCTGCCTAGCTTCCTCAGG-3' and 5'-CTTGGAGACATAGCCACACTG-3'. The primers used for the p44-Tg mice (Scrable, 2004) were: 5'-AAGCCTCGAAGTAAGTTGGATGCCTAG-3' and 5'-TGGCGGGATGTATCTTAAACCTTCC-3'. This master mix was added to 2 µl of template DNA, then placed into the thermocycler to undergo an appropriate PCR cycle. All PCRs were performed in a DNA Engine PTC 200. All PCR reactions were then run on a 1% agarose gel to determine the genotype of each mouse.

RT-qPCR

RNA Isolation from Liver, Muscle, and Fat Tissues

Total RNA from liver, muscle, and fat tissues were prepared using RNeasy kits (Qiagen) following the manufacturer's instructions. The purified RNA was subjected to

an additional DNase treatment (10 µl DNase and 70 µl DNase buffer, Ambion) to ensure removal of contaminating genomic DNA prior to final column purification. First and second elution RNA concentrations were read on a Thermo Nanodrop 2000 Spectrophotmeter. Purified RNA samples were frozen on dry ice and stored at -80°C.

RNA Clean-up

The RNA clean-up consisted of a DNase treatment (Ambion) followed by RNeasy kits (Qiagen), according to both manufacturer's instructions. 10 µg of the isolated RNA sample, in a total volume of 80 µl nuclease-free water, was added to a mix containing 2 µl DNase (Ambion), 10 µl 10X Buffer (Ambion), and 8 µl nuclease-free water. The samples were incubated for 20 minutes at 37°C, and then 1 µl DNase (Ambion) was added to each sample. The samples were incubated again for 20 minutes at 37°C, and then 10 µl inactivation buffer (Ambion) was added to each sample and mixed for 2 minutes at room temperature. The samples were spun at max speed for 2 minutes, and supernatants were transferred to a new tube; the RNeasy clean-up kit (Qiagen) instructions were then followed. Cleaned RNA samples were frozen on dry ice and stored at -80°C.

cDNA Synthesis

cDNA was prepared using Superscript III (Invitrogen) with random hexamers and 0.5 µg -1.0 µg of RNA per tissue, following the manufacturer's instructions for First-Strand cDNA Synthesis. cDNA samples were collected by brief centrifugation and stored at -20°C.

RT-qPCR

The relative expression of mRNA was examined by quantitative PCR analysis. Quantitative real-time PCR was performed on a Biorad Cycler using SyBr Green master mix (Biorad). The primer sequences for the murine genes are listed in below in **Table 1**. All samples were examined in triplicate, and values were normalized for baseline expression and for expression of *GAPDH*. Calculations of fold change were made using the ΔΔCt method. Statistical significance was calculated using CT values.

Table 1: Primers Used for Real Time RT-qPCR Analysis

Primers	**Strand**	**Code**
Gapdh	Sense	(5'-CTTCACCACCATGGAGAAGGC-3';
	Antisense	5'-GGCATGGACTGTGGTCAT-3')
Trp53	Sense	(5'-TGAAACGCCGACCTATCCTTA-3';
	Antisense	5'-GGCACAAACACGAACCTCAAA-3')
Mdm2	Sense	(5'-TGACACCAGAGCTTAGTCCTG-3';
	Antisense	5'-GCGTCTCGTAACGAATAAGGC-3')
Zfp385a	Sense	(5'-ACATTGAGCACCGCTATGTCT-3';
	Antisense	5'-CTCTCTTGGATGAGGGTCTGATA-3')
Sesn1	Sense	(5'- GTGGACCCAGAACGAGATGACGTGGC -3';
	Antisense	5'- GACACTGTGGAAGGCAGCTATGTGC -3')
Sesn2	Sense	(5'-TCCGAGTGCCATTCCGAGAT-3';
	Antisense	5'- TCCGGGTGTAGACCCATCAC-3')
Sesn3	Sense	(5'- GCGAGGAGAAGAACATTTGCC-3';
	Antisense	5'- CCAAACATACAGTGAACATAGT-3');
Sco2	Sense	(5'- GTGGACCCAGAACGAGATGACGTGGC-3';
	Antisense	5'-GACACTGTGGAAGGCAGCTATGTGC -3')

Immunoblots

Preparation of Tissue Protein Lysates

Animal tissues were homogenized in triton lysis buffer (1X triton lysis buffer (TLB, 20 mM Tris pH 7.4, 137 mM NaCl, 2 mM EDTA, 1% Triton lysis, 10% glycerol) containing protease and phosphatase inhibitors (5 µg/ml aprotinin, 5 mg/ml leupeptin, 5

mg/ml PMSF, 1 mM sodium orthovanadate, 25 mM beta-glycerophosphate). Protein samples were flash frozen in liquid nitrogen and stored at -80°C.

BCA Protein Assay

Protein samples and standards were prepared using the BCA Protein Assay Kit (Pierce) according to manufacturer's instructions. In each well, 2 µl of tissue lysate sample was added to 23 µl of sterile water, then 200 µl of working reagent was added to each sample well and mixed. The plate was incubated at 37°C for 30 minutes, and then the absorbance was read at 550 nm on a Thermo Multitask Ascent plate reader. The resulting concentrations were used to create the loading samples for the Western Blots. Each sample had 50 µg of protein in a total volume of 50 µl; 10 µl of Laemmli's SDS-sample buffer (6X, reducing) was added to the appropriate amount of protein sample and mixed well. 1X triton lysis buffer (TLB, 20 mM Tris pH 7.4, 137 mM NaCl, 2 mM EDTA, 1% Triton lysis, 10% glycerol, 5 mg/ml PMSF, 1 mM sodium orthovanadate, 25 mM beta-glycerophosphate) was added to each protein sample to bring the final total volume to 50 µl.

Immunoblot Analysis

Tissues extracts were examined by immunoblot analysis using primary antibodies to Akt and phospho-Ser473 Akt (Cell Signaling). 50-100 µg of cell extract were run on a 10% acrylamide gel with a 20% SDS buffer to separate proteins. Proteins were then blotted onto Immobolin-P (Biorad), using transfer buffer, following standard techniques. The membrane was blocked in a solution of TBS-T [TBS-T, 10 mM Tris pH 8.0, 150 mM NaCl, 0.05% Tween] with 10% skim milk for 1 hour. Primary antibodies (6 ml

TBS-T 10% milk with 6 µl of anti-phospho-AktSer472, Cell Signaling) were added to the membrane and incubated overnight at 4°C. The membrane was washed three times in TBS-T, for 5 minutes each time, and incubated with secondary antibodies (1:10,000 anti-mouse:block) for one hour. The membrane was washed again in TBS-T. Membranes were developed with chemilumenescence technique (GE Healthcare).

RESULTS

The purpose of this project was to assess the role of the p53 tumor suppressor pathway in maintaining glucose homeostasis. The ability to metabolize glucose and utilize insulin was monitored in two transgenic mouse models, a p53Ser23A mutant in which p53 cannot be phorphorylated at site 23, and an overexpression p44 model in which the activity of p53 is increased.

Mice Genotype and Phenotype

It was imperative to genotype all mouse strains, as this ensures correct breeding and strain conformation. The genotyping process started by sterilely cutting approximately 1 cm of each mouse tail, usually as they mice were weaned, and digesting the tail tissue to produce an aqueous solution from which DNA was isolated. The tail DNA was then isolated, and each mouse sample was analyzed by PCR. The PCR products were run on a 1% agarose gel and then analyzed to determine the genotype of each mouse. **Figure 10** is a photograph of mutant mice strains compared to WT mice DNA samples run on the gel to determine genotype. When looking at the p53Ser23A mutant mice gel (**Figure 10A),** a band at 280 bp indicates WT allele, and a band at 320 bp indicates a mutant allele; if these mice have both bands they are heterozygous p53Ser23A mutants, and if they have only one band, they are either homozygous WT or p53SerA depending on band location. In **Figure 10A,** Lane 4 is an example of WT (+/+), Lane 5 is an example of a heterozygous mutant (+/-), and Lane 6 is an example of a homozygous mutant (-/-). When looking at the p44 transgenic mice gel (**Figure 10B),** a band at 289 bp indicates that the p44 transgene is present; however this gel does not

allow for the distinction between hemizygous and homozygous mice. In **Figure 10B,** Lane 5 is an example of a transgenic mouse (either +/- or -/-), and Lane 6 is an example of a WT mouse (+/+).

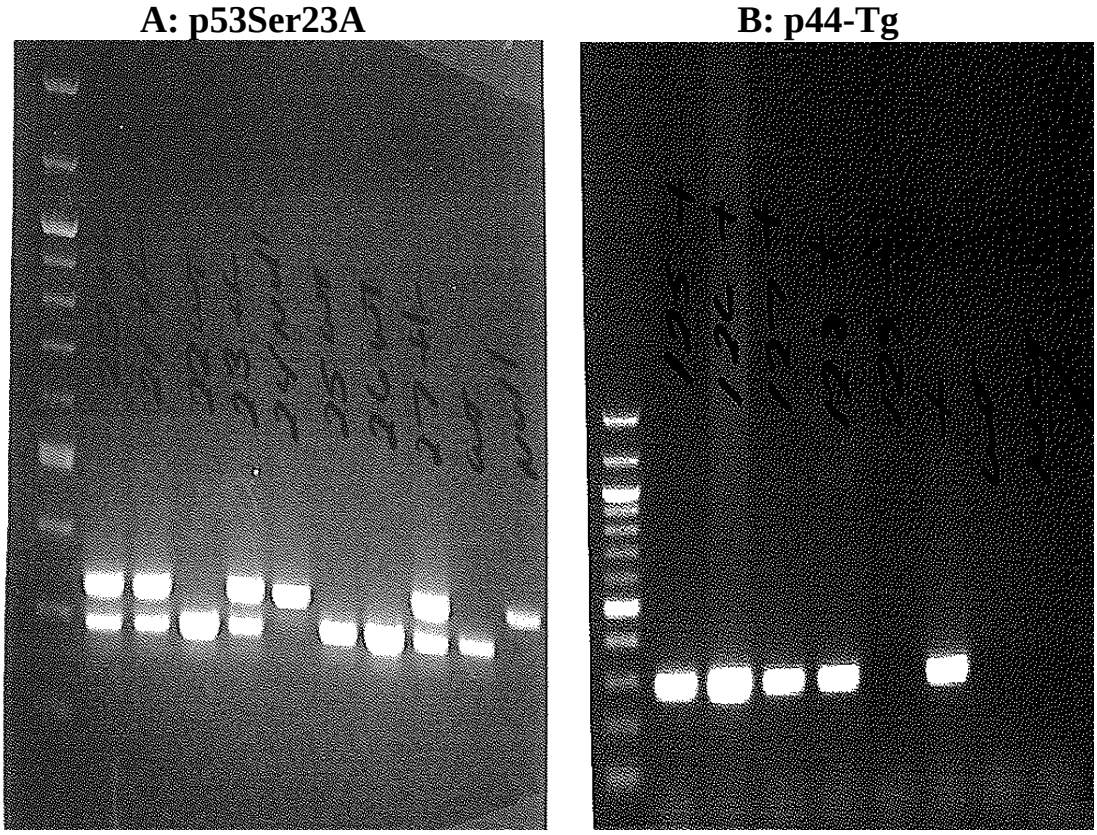

Figure 10. Gel of PCR Amplicons from Tail Digests for Genotyping Mutant and Wildtype Mice. (A) p53Ser23A mutant mice tail digest compared to wildtype mice. In 10A, the mutant mice are categorized as heterozygous (2 bands) or homozygous (1 band at 320 bp). In 10B, the transgenic mice are categorized as possessing the transgene if there is a band present.

The phenotype of each mouse strain can also be used to aid in the verification of the strain, especially in the p44-Tg mice. It is thought that p44 interacts with p53, affecting its ability to modulate gene expression and increasing its ability to suppress cell proliferation. Transgenic mice that overexpress p44 show signs of premature aging and are very small (Campisi, 2004). This is especially true in the homozygous p44-Tg mice, and these mice can almost always be accurately assessed based on size alone as they can

be half the size and weight of the WT mice. All of the mice used in the Glucose Tolerance Test (GTT) (and Insulin Tolerance Test ITT since the same mice were used) were weighed prior to experiments. The average weight of the eight p44-Tg mice used in the GTT and ITT experiments was 20% less than the average weight of the 17 WT mice used in the same GTT and ITT experiments, seen in **Table 2**. The p44-Tg were weighed (and tested) at an earlier age than the p53Ser23A mice as they had a lower life expectancy due to the hyperactivation of p53, which increased the rate of aging. **Table 2** also shows that the p53Ser23A mice were an average of 10% heavier than the WT strain; this is consistent with a high-fat body accumulation (Ikemoto et al., 1994).

Genotype	# Mice	Age	Weight (g)
Wildtype	**10**	**5 months**	**30**
p53Ser23A	**12**	**5 months**	**33**
Wildtype	**17**	**3 months**	**30**
p44-Tg	**8**	**3 months**	**24**

Table 2. Average Weights of the p53Ser23A and p44-Tg Mice Compared to WT Mice. Wildtype and p53Ser23A mice were weighed at 5 months, while p44-Tg mice were weighed at 3 months due to their early death rates. p53Ser23A mice weighed 10% more than the WT, which is consist with a high-fat body weight leading to a pre-diabetic state. The p44-Tg weighed 20% less than the WT because the homozygous phenotype of this model is characterized by a smaller body size.

Analysis of p44 Transgenic Mice

The p44 transgenic mice and WT mice were subjected to a Glucose Tolerance Test (GTT) and an Insulin Tolerance Test (ITT) at 3 months of age. The GTT (**Figure 11**) was performed 1 week before the ITT (**Figure 12**). Prior to the GTT, the mice were

fasted overnight. Glucose (1g/kg body weight, IMS) was administered via an intraperitoneal injection, and blood glucose levels were measured with a an Ascenzia Breeze 2 glucometer (Bayer) at 0, 15, 30, 45, 60 and 120 min after glucose stimulation. The blood was drawn from a tail cut made at the start of the GTT. The determined glucose levels were graphed and analyzed to assess whether glucose intolerance occurs in the p44-Tg mice. The GTT is an essential test for diabetes research involving mouse models as it is the only means of identifying impaired glucose tolerance (Andrikopoulous et al., 2008). The GTT measures the animal's ability to metabolize glucose. The GTT starts with an i.p. injection of glucose, causing glucose levels in the body to dramatically increase. The body should release insulin in response to this increased glucose level. The amount of blood glucose should increase immediately, as glucose is absorbed into the body and then decrease as the secreted insulin helps converts glucose to glycogen. At 120 minutes post administration of glucose, the blood glucose levels should return to basal levels (assumed by the WT blood glucose level at t= 120 minutes).

The p44 transgenic mice were found to exhibit glucose intolerance compared to the wildtype mice (**Figure 11**). This is seen in the elevated *basal* glucose levels, as WT mice had approximately 90 mg/dL basal glucose, while p44-Tg mice showed approximately 125 mg/dL glucose. As expected, the blood glucose levels increased significantly at t= 15 minutes post-injection. Post administration of glucose, the p44-Tg mice blood glucose levels increased to a greater level than the WT mice. Although the p44-Tg mice blood glucose levels decreased over time, they consistently remained above the WT levels. Statistically significant differences ($P<0.05$) between the glucose levels in

the WT mice and transgenic mice occurred at t= 0 and t=15 minutes after glucose stimulation (denoted by asterisks in the figure).

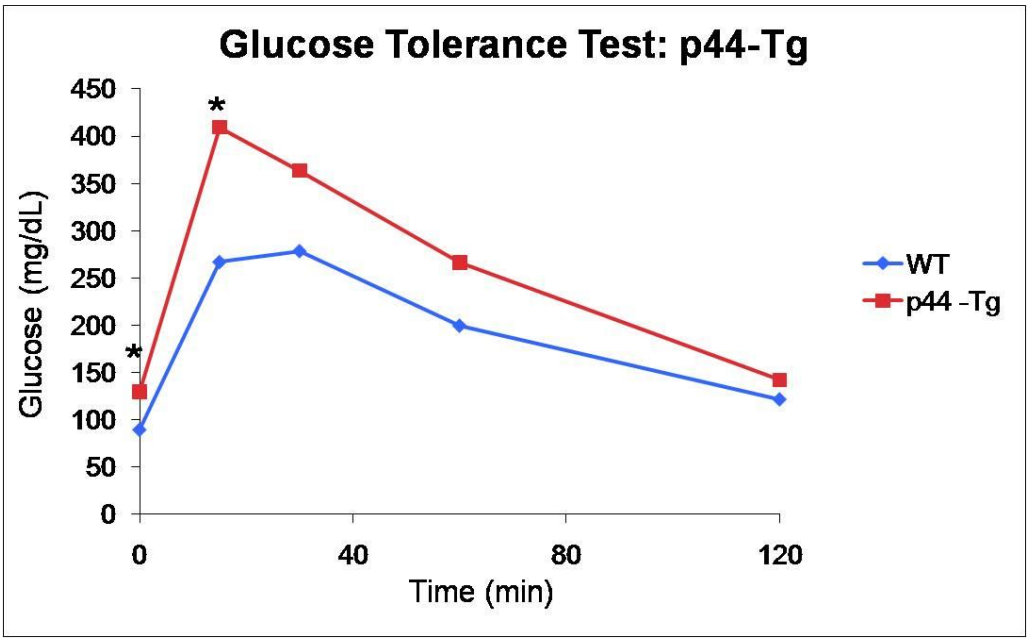

Figure 11. ***In Vivo*** **Glucose Tolerance Test for p44-Tg Mice Compared to WT Mice**. The GTT showed that the p44 transgenic mouse showed glucose intolerance compared to the wildtype mice, illustrated by the slightly elevated basal glucose levels, and a significant increase in glucose levels at t= 15 minutes. Statistically significant differences between glucose levels of the WT and transgenic mice strains are indicated (*, $P < 0.05$).

The insulin tolerance test (ITT) was performed one week after the glucose tolerance test on the same p44-Tg and WT mice. Prior to the start of the ITT, the mice were not fasted overnight; The time = 0 minutes glucose reading was taken before the stimulation with insulin from a tail cut, making this time point an indication of basal level glucose. The insulin (0.75 units/kg body weight, Sigma, St. Louis, MO) was administered via an intraperitoneal injection, and blood glucose levels were measured from the tail cut with a an Ascenzia Breeze 2 glucometer (Bayer) at 15, 30, 60, 90 and 120 min after insulin stimulation. The determined blood glucose levels were graphed and analyzed to assess whether insulin resistance occurs in the p44-Tg mice. The administration of insulin

decreases serum glucose; the ITT measures the body's ability to utilize insulin. In the presence of insulin, the body should stop the breakdown of glycogen into glucose in the liver, and initiate the transformation of glucose into glycogen, thus the blood glucose levels should decrease in the presence of insulin. The large amount of injected insulin should induce hypoglycemia. As homeostasis is achieved in the body, the blood glucose measurements should level off in a straight line. Since the t=0 glucose reading was taken prior to insulin stimulation, this reading can be used as a basal level.

The p44 transgenic mice showed insulin *sensitivity* compared to the wildtype mice (**Figure 12**), despite their elevated basal glucose levels. Both the wildtype and transgenic mice exhibited elevated basal glucose readings (above 126 mg/dL), though this could be because the mice had eaten right before the start of the ITT as they were not starved overnight. Glucose levels decreased by almost twice the amount in p44-Tg mice compared to wildtype mice (WT mice dropped 71.65 mg/dL, while p44-Tg mice dropped 134.0 mg/dL). After the steep decrease in glucose levels, the p44-Tg glucose levels began to increase. Unlike the WT mice, who's glucose measurements leveled off (creating a linear line), the p44-Tg mice glucose measurements kept increasing. Though the WT and p44-Tg mice ended with similar glucose levels, the p4-Tg mice had an increasing slope, meaning the insulin and glucose levels were not reaching a homeostasis; instead the glucose levels were increasing. The t= 120 minutes post insulin stimulation had the second highest glucose level. Based on this quick, large drop in glucose levels, coupled with increasing (not steady) glucose levels, the p44-Tg animals appear to be more insulin *sensitive* than the WT mice, and suggests that the p44-Tg mice have an insulin/Akt pathway in which the pathway stimulation is impaired. The statistically significant

differences ($P < 0.05$) between glucose levels of the WT and transgenic mice strains occurred at t=0 minutes (shown as an asterisk).

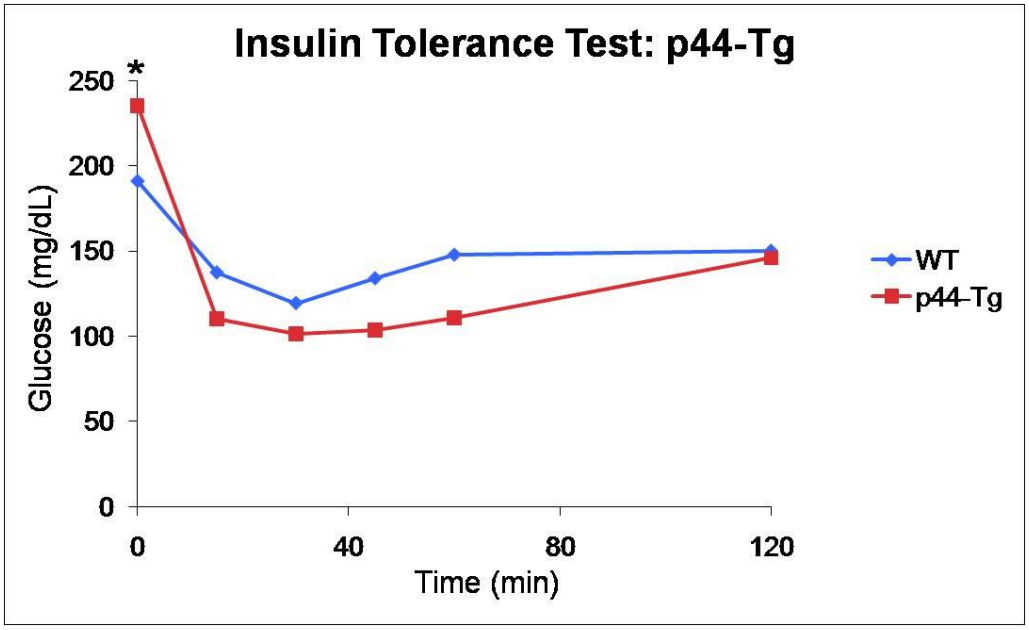

Figure 12. ***In Vivo*** **Insulin Tolerance Test for p44-Tg Mice Compared to WT Mice**. Although basal glucose levels are elevated in the p44-Tg model, these mice are still sensitive to insulin. Glucose levels decreased by almost twice the amount in p44-Tg mice compared to wildtype mice (WT mice dropped 71.65 mg/dL, while p44-Tg mice dropped 134.0 mg/dL). Therefore, the p44-Tg animals are more insulin sensitive. Statistically significant differences between glucose levels of the WT and transgenic mice strains are indicated (*, $P < 0.05$).

Analysis of p53Ser23A Mutant Mice

The p53Ser23A mutant mice and WT mice were subjected to a Glucose Tolerance Test and an Insulin Tolerance Test at 5 months of age. The GTT (**Figure 13**) was performed 1 week before the ITT (**Figure 14**). Prior to the GTT, the mice were fasted overnight. The glucose (1g/kg body weight, IMS) was administered via an intraperitoneal injection, and blood glucose levels were measured with a an Ascenzia Breeze 2 glucometer (Bayer) at 0, 15, 30, 45, 60 and 120 min after glucose stimulation. The blood was drawn from a tail cut made at the start of the GTT. The determined blood glucose

levels were graphed and analyzed to assess if glucose intolerance occurs in the p53Ser23A mutant mice.

The p53Ser23A mutant mice exhibited glucose intolerance compared to the wildtype mice (**Figure 13**). The p53Ser23A mutant mice glucose levels increased to a much higher point than the WT mice, but the glucose was converted into glycogen as seen in the final glucose measurement, as the WT and p53Ser23A levels were almost equal. The glucose intolerance exhibited by the p53Ser23A mutant mice is clearly exhibited by the significantly increased glucose levels at t=15 and t= 30 minutes post glucose stimulation. These time points are the statistically significant differences ($P<0.05$) between the glucose levels in the WT mice and mutant mice.

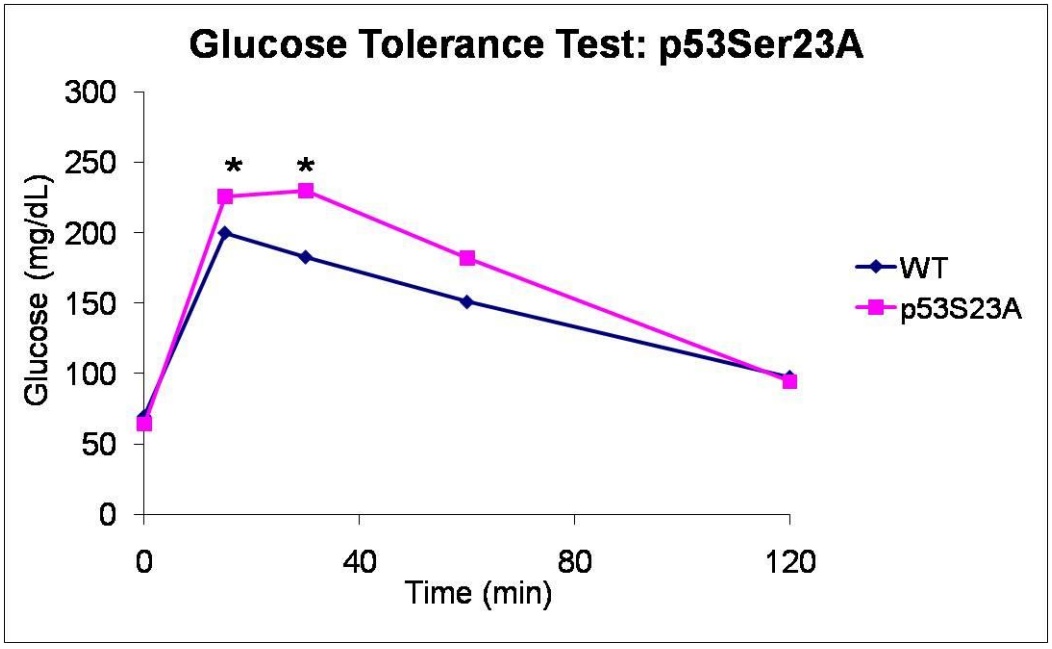

Figure 13. *In Vivo* Glucose Tolerance Test for p53Ser23A Mice Compared to WT Mice. The p53Ser23A GTT showed that p53Ser23A mouse mutant exhibited elevated glucose intolerance compared to the wildtype mice shown by the significantly increased glucose levels. Statistically significant differences between glucose levels of the WT and the p53Ser23A mutant mice strains are indicated (*, $P < 0.05$).

The insulin tolerance test was performed one week after the glucose tolerance test on the same p53Ser23A mutant and WT mice. Prior to the start of the ITT, the mice were fasted overnight. A time = 0 minutes basal glucose level was taken before the stimulation with insulin from a tail cut. The insulin (0.75 units/kg body weight, Sigma, St. Louis, MO) was administered via an intraperitoneal inject, and blood glucose levels were measured from the tail cut with a an Ascenzia Breeze 2 glucometer (Bayer) at 15, 30, 60, 90 and 120 min after insulin stimulation. The determined glucose levels were graphed and analyzed to assess whether insulin resistance occurs in the p53Ser23A mutant mice.

As was observed with the p44 mice, the p53Ser23A mutant mice exhibited insulin sensitivity when compared to the wildtype mice (**Figure 14**). In this case the initial drop in glucose levels was identical between WT and p53Ser23A mice. Unlike the p44 mice, where the difference in glucose drop was used to declare insulin sensitivity, the insulin sensitivity in the p53Ser23A mice rests in the rapid return to glucose levels equal to the glucose levels before the insulin injection. The glucose levels in the p53Ser23Ala mutant mice initially decreased, but then steadily increased, and at t=120 minutes post insulin stimulation, the glucose levels were equal to basal level glucose readings, showing the mutant mice to be in a state of hyperglycemia relative to WT mice (although the actual final serum glucose level of approximately 90 mg/dL falls within the norm for mice of 72 to 126 mg/dL). The insulin sensitivity in the p53Ser23A mutant mice is characterized by rapidly elevated glucose levels, compared to the wildtype mice, that were unable to return to basal glucose levels (remaining at 97 mg/dL); thus, the p53Ser23A mutant animals are more insulin sensitive than the WT strain. The statistically significant differences ($P <$

0.05) between glucose levels of the WT and mutant mice strains occurred at t= 60 , t=90, and t= 120 minutes post insulin stimulation.

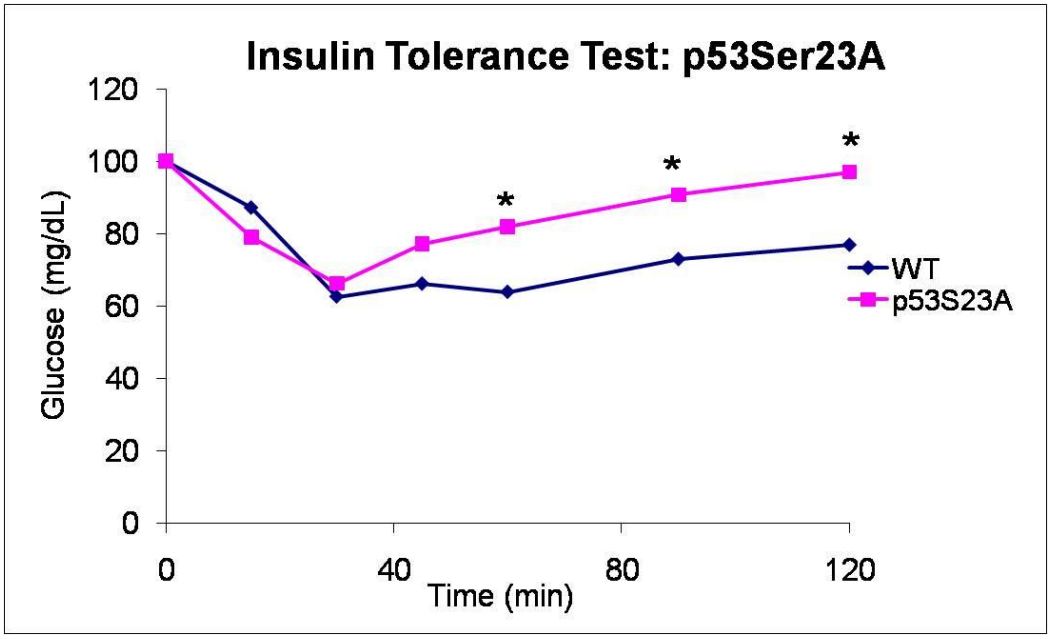

Figure 14. ***In Vivo*** **Insulin Tolerance Test for p53Ser23A Mice Compared to WT Mice.** The p53Ser23A ITT showed that the mutant animals exhibited glucose levels that became rapidly elevated, compared to the wildtype mice, and were unable to return to basal glucose levels (remaining at 97 mg/dL); thus, the p53Ser23A mutant animals are more insulin sensitive than the WT strain. Statistically significant differences between glucose levels of the WT and the p53Ser23A mutant mice strains are indicated (*, $P < 0.05$).

The relative expression of the p53-inducible *sestrin* gene in WT mouse and p53Ser23a mouse liver was determined through an Real-Time Polymerase Chain Reaction (RT-qPCR). Highly conserved and p53-inducible, the *sestrin* gene occurs in three forms: *sestrin 1, sestrin 2, and sestrin 3*. The relative expression of sestrin (*sesn*) in the liver serves as a control to the functionality of p53. Wildtype p53 is functional, and thus it should induce high levels of all three *sesn* proteins, as it does in **Figure 15** (WT represented by the blue bar)**.** This shows that the WT has a functional p53 domain. The p53Ser23A mutant should show decreased levels of *sesn* activity since the *serine23*

phosphorylation site has been mutated into an *alanine*. This seems to be true in the in **Figure 15**, though none of the difference in relative expression of *sesn 1, sesn 2,* or *sesn 3* are statistically important ($P < 0.05$). It was discovered that the *sesn* standards used in this RT-qPCR were old and therefore not expressing true levels of protein.

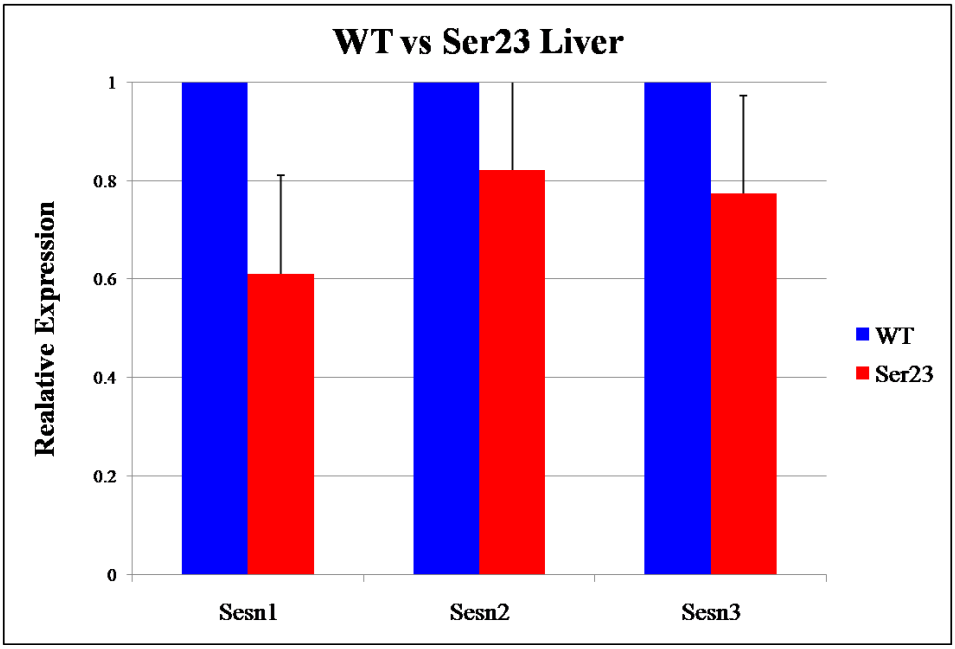

Figure 15. RT-PCR Analysis of the Relative *Sestrin* Gene Expression in the Liver of WT and p53Ser23A Mice. Expression was measured by quantitative RT-PCR (mean ± S.E.M.; n = 3). *Sestrins* are highly conserved p53-inducible proteins and may play a role in regulating ROS levels. The relative expression was corrected for the amount of *Gapdh* mRNA in each sample and was normalized to a value of 1 for wild-type mice. There are no statistically significant differences between WT and p53Ser23A mice ($P < 0.05$).

Insulin Signaling Pathway

Since insulin functions are the principal facet of glucose metabolism and the development of Type 2 diabetes, the efficacy of the insulin signaling pathway was studied. Studying the wildtype mice strain for an understanding of how the Akt pathway functions in response to insulin is necessary for a control (see **Figure 16**). This was achieved by treating WT liver and muscle with insulin to phosphorylate the Akt Ser473

site, which activates the Akt pathway. These samples were then examined via immunoblot analysis.

In liver and muscle in the presence of insulin, Akt was found to be active, showing an increase in the band intensity for Ser473 phosphorylation, while the intensities of total Akt (lower panel) were approximately equal. In the absence of insulin, less phosphorylated Akt was observed, as this shows the Akt proteins are present but not phosphorylated. Not analyzed was Akt activation in tissues of p53Ser23A and p44-Tg mice as a method for investigating the insulin signaling pathway.

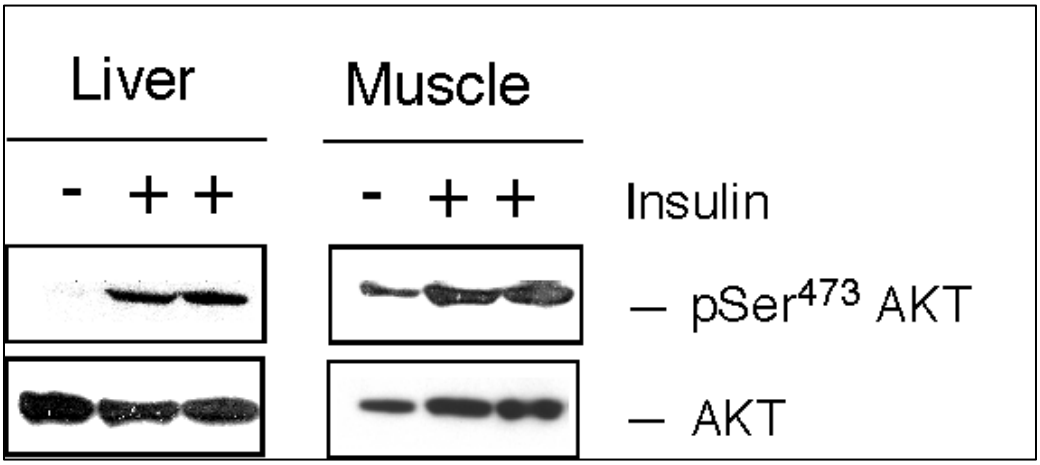

Figure 16. Insulin Signaling in p53 Wildtype Liver and Muscle Tissues. Activation of Akt in wildtype liver and muscle in response to insulin was analyzed by immunoblot analysis. *Ser*^{473} phosphorylation was used as a measaure of Akt activation , and was induced in the liver and muscle in response to insulin treatment.

DISCUSSION

The purpose of this project was to assess the role of the p53 tumor suppressor pathway in maintaining glucose homeostasis. Two mouse models, a "knock down" p53Ser23A mutant strain in which the p53 Ser23 site can not be phosphoryated, and an overexpression p44 transgenic strain showing increased p53 activity, were studied to analyze the role of p53 in glucose homeostasis. Both strains exhibited signs of glucose intolerance and insulin sensitivity, though in the p44-Tg strain the glucose intolerance was more pronounced than the insulin sensitivity, and in the p53Ser23A strain the insulin sensitivity was more pronounced than the glucose intolerance.

The p44 transgenic strain's GTT exhibited glucose levels that increased to a much higher point than the WT strain did. The glucose levels decreased over time, but they remained elevated compared to the WT glucose levels. This elevation of glucose is what characterizes the p44-Tg mice glucose intolerance. The ITT showed that the p44-Tg mice were insulin sensitive. The elevated basal glucose levels in the mice indicate that there could be a problem with the insulin/Akt pathway because there is an abnormally high blood glucose level (leading to a state of hyperglycemia) indicating that insulin is not initiating the conversion of glucose to glycogen. Once these mice were challenged with insulin, the glucose levels dropped, showing that the insulin receptors are still functioning, though not as they should be. It could also mean that the p44-Tg mice are not producing enough insulin. This could explain the unusually high basal glucose levels and why the glucose levels decreased when challenged by insulin. Once the glucose was being converted into glycogen, the blood glucose levels dropped, but they dropped too

low, indicating the body is unable to regulate insulin production and glucose metabolism because it is unable to reach homeostasis. The decrease in glucose levels in the p44-Tg mice was almost double the drop seen in the WT mice. After the glucose levels dipped they started increasing, not leveling off as would be expected if homeostasis was achieved (this linear leveling off can be seen in the WT mice). It seemed that the glucose levels were increasing continually, and the final time point, t= 2 hours post insulin administration was the second highest time point. This suggests that the p44 transgenic mice have an impaired insulin/Akt pathway.

The p53Ser23A mutant mice glucose tolerance test showed that these mice exhibited glucose intolerance. The glucose levels raised to a higher point than in the WT mice, but were able to stabilize at a glucose measurement comparable to the WT's final glucose reading, indicating glucose homeostasis was achieved. The increased glucose readings imply that these mice were unable to convert glucose to glycogen as efficiently as the WT mice could. The p53Ser23A mutant mice ITT showed that these mice exhibit insulin sensitivity. The ITT showed that the glucose levels decreased in response to the administration of insulin, but then steadily increased, indicating that the insulin was able to initiate the conversion of glucose to glycogen, but the effect was short-lasted. The glucose levels increased after t= 30 minutes post insulin stimulation, and continued to increase; at t= 120 minutes post insulin stimulation, glucose levels were equal to basal glucose levels, and the p53Ser23A mice were in a state of hyperglycemia.

Both the p53Ser23A mutation, a "knockdown" of p53 and the p44 transgene that overexpresses p53, showed glucose intolerance and insulin sensitivity. The knockdown

mutation showed a greater insulin sensitivity than glucose intolerance, indicating that these mice could have an impaired insulin receptors because these mice do not seem able to utilize insulin to convert glucose to glycogen. The p53Ser23A mice did not exhibit an elevated basal glucose level, indicating the mice are able to maintain glucose homeostasis. The GTT showed the mutant mice were able to convert glucose to glycogen, but at a slower rate; thus the p53Ser23A mice are able to utilize insulin to convert glucose to glycogen, but at an impaired rate compared to the wildtype mice. The p44 transgenic mice cause an overexpression of p53 in these animals; when p53 is overexpressed, these mice were more glucose intolerant than insulin sensitive. When the p44-Tg mice were challenged with glucose, their blood glucose levels skyrocketed to over 400 mg/dL, while the wildtype mice remained around 250 mg/dL. This severe increase in glucose levels indicate the mice are unable to produce enough insulin to respond to the administered glucose, or, if the mice are producing insulin, their insulin receptors (or Akt pathway) or non-functional. The elevated basal glucose levels, illustrated on the ITT, correspond to this idea because this shows the mice are unable to regulate glucose levels.

The exact function of the p53 tumor suppressor pathway in maintaining glucose homeostasis remains unknown, but altering its functions in any manner has an effect on glucose homeostasis, indicating that p53 does play a role. The two mouse models utilized in this project, the "knockdown" model of the Ser23 phosphorylation site and the overexpression of p53 through p44 alter the functions of p53 in opposing ways, therefore it was expected that the results from these polar models would reflect this contrast. However, this was not the case as both mouse models resulted in glucose intolerance and

insulin sensitivity, though in differing degrees. This outcome illustrates the complexity of both the insulin signaling pathway and the functions of p53. Further tests studying the p53Ser23A mutation and the p44 transgenic strain need to be completed for a more complete understanding of the p53 tumor suppression pathway's role in glucose homeostasis. Specifically, these tests should include a continuation of the RT-qPCRs (to show relative protein expression to test for the functionality of p53) and western blots (to test the functionality of the Akt pathway). Also, other members of the insulin signaling pathway could be monitored for activity to determine whether the alteration in p53 activity affects their activation.

BIBLIOGRAPHY

American Diabetes Association (2010) "Diabetes Basics." American Diabetes Association, 2010. Web. 06 Apr 2010. <http://www.diabetes.org/diabetes-basics/type-2/>.

Andrikopoulous, S, Blair, A, Deluca, N, Fam, B, Proietto, J. 2008. Evaluating the glucose tolerance test in mice. *American Journal of Physiology-Endocrinology and Metabolism*, **295**(6): 1323-1332.

Bar, R.S. et al. 1978. Extreme insulin resistance in ataxia telangiectasia: defect in affinity of insulin receptors. The *New England Journal of Medicine,* **298**, 1164-1171.

Campisi, J. 2004. Fagile fugue: p53 in aging, cancer and IGF signaling. *Nature Medicine*, **3**(10): 231-232.

Garcia, F, Zalba, G, Paez, G, Encio, I, de Miguel, C. 1998. Molecular cloning and characterization of the human p44 mitogen-activated protein kinase gene. *Genomics*, **50**(1): 69-78.

Ikemoto, S, Thompson, K, Takahashi, M, Itakura, H, Lane, D, Ezaki, O. 1995. High fat diet-induced hyperglycemia: Prevention by low level expression of a glucose transporter (GLUT4) mini in transgenic mice. *Proceedings of the National Academy of Sciences*, **92**(8): 3096-3099.

Kahn, C. R., Saltiel, A. R., 2001. Insulin signaling and the regulation of glucose and lipid metabolism. *Nature,* **414:** 799-806.

Kubbutat, M. H., Jones, S. N., and Vousden, K. H. 1997. Regulation of p53 stability by Mdm2. *Nature,* **387** (6630): 299-303.

Lavin, M.F. 2008. Ataxia-telangiectasia: from a rare disorder to a paradigm for cell signalling and cancer. *Nature Reviews Moleclar Cell Biology*, **9**, 759-69.

Luo, J., Li, M., Tang, Y., Laszkowska, M., Roeder, R. G., and Gu, W. 2004. Acetylation of p53 augments its site-specific DNA binding both *in vitro* and *in vivo. Proceedings of the National Academy of Sciences*, **101**(8): 2259-2264.

Macpherson, D., Kim, J., Kim, T., Rhee, B. K., Van Oostrom, C. T., Ditullio, R. A., Venere, M., Halazonetis, T. D., Bronson, R., De Vries, A., Fleming, M., and Jacks. 2004. Defective apoptosis and B-cell lymphomas in mice with p53 point mutation at Ser 23. *The Embo Journal*, **23**(18): 3689-3699.

Maier B, Gluba W, Bernier B, Turner T, Mohammad K, Guise T, Sutherland A, Thorner M, Scrable H. 2004. Modulation of mammalian life span by the short isoform of p53. *Genes and Development*, **18**: 306–319.

Manning, B., Cantley, L. 2007. AKT/PKB Signaling: Navigating Downstream. *Cell*, **129**(7): 1261-1274.

Ogawa. W., Matozaki T., Kasuga M. 1998. Role of binding proteins to IRS-1 in insulin signaling. *Molecular and Cellular Biochemistry*, **182**: 13-22.

Olovnikov, I. A., Kravchenko, J. E., Chumakov, P. M. 2008. Homeostatic functions of the p53 tumor suppressor: Regulation of energy metabolism and antioxidant defense. *Seminars in Cancer Biology*. **19**: 32-41.

Rudolph, K. L.Chang, S.Lee, H. W.Blasco, M.Gottlieb, G. J.Greider, C.DePinho, R. A. 1999. Longevity, stress response, and cancer in aging telomerase-deficient mice. *Cell*, **96:** 701-712.

SABiosciences. (2009) "Insulin Receptor Pathway." SABiosciences, A Qiagen Company, 2009. Web. 24 Apr 2010. <http://www.sabiosciences.com/pathway.php?sn= Insulin_Receptor_Pathway>.

Schmitt, C. A., Mccurrach, M. E., De Stanchina, E., Wallace-Brodeur, R. R., and Lowe, S. W. 1999. INK4a/ARF mutations accelerate lymphomagenesis and promote chemoresistance by disabling p53. *Genes and Development*, **13**(20): 2670-2677.

Scrable H, Sasaki T, Maier B. 2005. DeltaNp53 or p44: priming the p53 pump. *The International Journal of Biochemistry and Cell Biology*, **37**: 913–919.

Shoelson, S.E. 2006. Banking on ATM as a new target in metabolic syndrome. *Cell Metabolism*, **4**: 337-338.

Sluss, H.K., Armata, H., Gallant, J. & Jones, S.N. 2004. Phosphorylation of serine 18 regulates distinct p53 functions in mice. *Molecular and Cellular Biology*, **24**(3): 976-984.

Spring, K., Ahangari, F., Scott, S. P., Waring, P., Purdie, D. M., Chen, P. C., Hourigan, K., Ramsay, J., Mckinnon, P. J., Swift, M., and Lavin, M. F. 2002. Mice heterozygous for mutation in Atm, the gene involved in ataxia-telangiectasia, have heightened susceptibility to cancer. *Nature Genetics*, **32**: 185-190.

Steele, R. J., Thompson, A. M., Hall, P. A., and Lane, D. P. 1998. The p53 tumour suppressor gene. *British Journal of Surgery*, **85**(11): 1460-1467.

Whiteman, E. L., Cho, H., Birnbaum, M. J. 2002. Role of Akt/protein kinase B in metabolism. *TRENDS in Endocrinology and Metabolism*, **13**(10): 444-451.